Recent Trends in the Study of Compact Objects: Theory and Observation
ASI Conference Series, 2013, Vol. 8, pp 51–54
Edited by Santabrata Das, Anuj Nandi and Indranil Chattopadhyay

Compton cooling and its effects on spectral and hydrodynamic properties of an accretion flow around a black hole: results of a coupled monte carlo TVD simulation

H. Ghosh[1*], S. K. Garain[2] and S. K. Chakrabarti[1,2]

[1]*Indian Centre for Space Physics, Chalantika 43, Garia Station Road, Kolkata 700084*
[2]*S N Bose National Centre for Basic Sciences, Salt Lake, Kolkata 700098*

Abstract. We investigate the effects of cooling of the Compton cloud on the outflow formation rate in an accretion disk around a black hole using a time-dependent coupled hydrodynamics - radiative transfer sumulation. We show that as a result of inverse-Comptonization of the soft photons, originating from the Keplerian disk immersed into an accreting sub-Keplerian flow (halo), by the hot Compton cloud, the cloud becomes cooler with the increase in the disk rate. As the resultant thermal pressure is reduced, the post-shock region collapses and the outflow rate is also reduced. We also find a direct correlation between the spectral states and the outflow rates of an accreting black hole.

Keywords : black holes: accretion – black holes: radiative transfer – methods: numerical

1. Introduction

It is generally believed that the outflows and jets in a compact binary system containing black holes originate from the accretion disk itself (Chattopadhyay et al. 2004 and references therein). Assuming the most general accretion flow configuration, namely, two-component advective flow (TCAF) model (Chakrabarti & Titarchuk 1995), in this paper, while computing the time variation of the velocity components, density, and temperature, we also compute the temporal dependence of the spectral properties. As a result, we not only compute the outflow properties, but also correlate them with the spectral properties.

*email: ehimadri@gmail.com / himadri@csp.res.in

2. Simulation set up and procedure

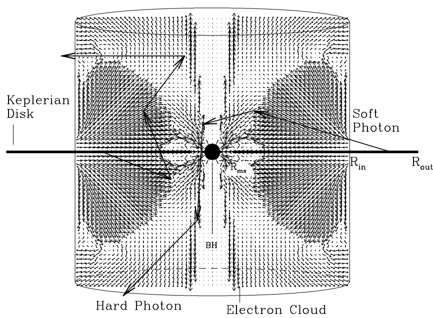

Figure 1. Schematic diagram of the geometry of our Monte Carlo simulations. Zigzag trajectories are the typical paths followed by the photons. The velocity vectors of the infalling matter inside the cloud are shown. The velocity vectors are plotted for $\lambda = 1.73$ and $\epsilon = 0.0021$.

In Fig. 1, the schematic diagram of our simulation set up is presented. The outer boundary of the sub-Keplerian matter is at $R_{in} = 100r_g$ ($r_g = \frac{2GM}{c^2}$) whereas that of the Keplerian disk at the equatorial plane is located at $R_{out} = 200r_g$. At the center, a non-rotating black hole of mass $10M_\odot$ is located. The sub-Keplerian flow dynamics is simulated using a TVD code. The details of this code can be found in Molteni, Ryu & Chakrabarti (1996) and Giri, Chakrabarti, Samanta & Ryu (2010). For a particular simulation, we use the Keplerian disk rate ($\dot{m}_d$) and the sub-Keplerian halo rate ($\dot{m}_h$) as parameters. The specific energy (ϵ) and the specific angular momentum (λ) determines the hydrodynamics (shock location, number density and velocity variations etc.) and the thermal properties of the sub-Keplerian matter. The radiative properties of the accretion disk is studied using a Monte Carlo code (Poznyakov, Sobol & Sunyaev 1983; Ghosh, Chakrabarti & Laurent 2009). The hydrodynamic code and the radiative transfer code are coupled together and are run back to back. The details of the coupling procedure and the equations used can be found in Ghosh, Garain, Giri & Chakrabarti (2011) and Garain, Ghosh & Chakrabarti (2012).

3. Results and discussions

Table 1: Parameters used for the simulations.

Case	ϵ, λ	$\dot{m}_h$	$\dot{m}_d$
Ia	0.0021, 1.73	1.0	No Disk
Ib	0.0021, 1.73	1.0	0.5
Ic	0.0021, 1.73	1.0	1.0
Id	0.0021, 1.73	1.0	2.0

In Table 1, we list various Cases with all the simulation parameters used in the present paper. The specific energy (ϵ) and specific angular momentum (λ) of the sub-Keplerian halo are given in Column 2. Columns 3 and 4 give the halo ($\dot{m}_h$) and the disk ($\dot{m}_d$) accretion rates. The corresponding cases are marked in Column 1. In Case

Ia, no Keplerian disk was placed in the equatorial plane of the halo, so in this case no Compton cooing is included.

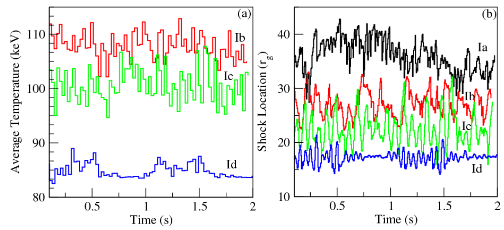

Figure 2. Time variation of the average temperature (keV) of the post shock region (a) and the location of the shock (in r_g) at the equatorial plane (b) for different cases (marked on each curve). See text for details.

In Fig. 2(a) we plot the average temperatures of the post-shock region only for those cases where the cooling due to Comptonization is included (Cases I(b-d)). The average temperature was obtained by the optical depth weighted averaging procedure prescribed in (Chakrabarti & Titarchuk 1995). The average temperature in the post-shock region is reduced rapidly as the supply of the soft photons is increased. In Fig. 2(b), we present the time variation of the shock location (in units of r_g) for various Cases (marked on each curve) given in Table 1. All the solutions exhibit oscillatory shocks. For no cooling, the shock is produced at a higher radius, as the cooling is increased the average shock location decreases since the cooling reduces the post-shock thermal pressure and the shock could not be sustained till higher thermal pressure is achieved at a smaller radius. The corresponding oscillations are also suppressed.

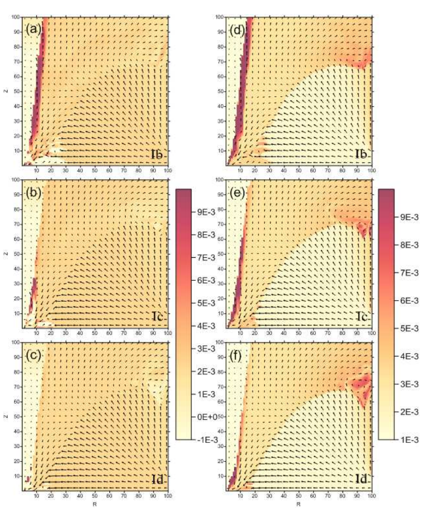

Figure 3. Color map of final specific energy (a-c) and entropy ($K = \frac{p}{\rho^\gamma}$) (d-f) distribution inside the accretion disk for different disk rates. The high-energy, high-entropy matter (dark zone, dark red online) are ejected outward as a hollow jet. The high-energy, high-entropy outflow decreases with the increase in disk rate. Velocity vectors at the injection boundary on the right is of length 0.05.

In Fig. 3(a-c), we present the specific energy distribution (left panel) for all the cooling Cases (marked in each box) at the end of our simulation. The velocity vectors are also plotted. The left scale gives the specific energy. We note that lesser and lesser amount of matter has higher energy as the cooling is increased. A similar observation could be made from the Fig. 3(d-f), where the entropy distribution is plotted. The jet matter having upward pointing vectors have higher entropy. However, this region shrinks with the increase in Keplerian rate, as the cooling becomes significant the outward thermal drive

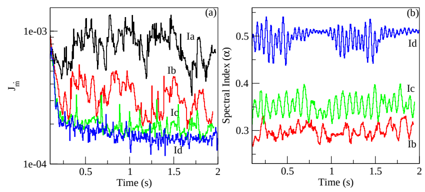

Figure 4. (a) Variations of $J_{\dot{m}}$ with time for different $\dot{m}_d$ is shown here. (b) Time variation of the spectral slope for different disk rates are shown. The Cases are marked in each curve. See text for detail.

To quantify the outflow rate let us take only those matter which have high positive energy and high entropy. Thus, we concentrate only on matter outflowing within $r = 20r_g$ at the upper boundary of our computational grid. We define this to be $J_{\dot{m}}$ $(= \frac{\dot{M}_{jet}}{\dot{M}_{in}})$. Fig. 4a shows time variation of $J_{\dot{m}}$. This outflow rate fluctuates with time. We find that the cooling process reduces this high energy component of matter drastically. Thus both the slow moving outflows and fast moving jets are affected by the Comptonization process at the base. In Fig. 4b, time variation of the spectral slope is shown. We find that spectrum becomes softer as $\dot{m}_d$ increases keeping $\dot{m}_h$ fixed. Thus we find that the outflow rate reduces when the spectrum becomes softer.

The work of HG was supported by a grant from Ministry of Earth Science.

References

Chattopadhyay I., Das S., Chakrabarti S. K., 2004, MNRAS, 348, 846
Chakrabarti S. K., Titarchuk L. G., 1995, ApJ, 455, 623
Molteni D., Ryu D., Chakrabarti S. K., 1996, ApJ, 470, 460
Giri K., Chakrabarti S. K., Samanta M. M., Ryu D., 2010, MNRAS, 403, 516
Poznyakov, L., Sobol, I., Sunyaev, R., 1983, A & Sp Physics Reviews, 2, 189
Ghosh H., Chakrabarti S. K., Laurent P., 2009, IJMPD, 18, 1693
Ghosh H., Garain S. K., Giri K., Chakrabarti S. K., 2011, MNRAS, 416, 959
Garain S. K., Ghosh H., Chakrabarti S. K., 2012, ApJ, 758, 114